

1 Article

## 2 Improving parametric cyclonic wind fields using 3 recent satellite remote sensing data

4 Yann Krien <sup>1,\*</sup>, Gaël Arnaud <sup>1</sup>, Raphaël Cécé <sup>1</sup>, Jamal Khan <sup>2,3</sup>, Ali Bel Madani <sup>4</sup>, Didier Bernard <sup>1</sup>,  
5 A.K.M.S. Islam <sup>3</sup>, Fabien Durand <sup>2</sup>, Laurent Testut <sup>5</sup>, Philippe Palany <sup>4</sup> and Narcisse Zahibo <sup>1</sup>

6 <sup>1</sup> LARGE, University of the French West Indies, Guadeloupe, France

7 <sup>2</sup> LEGOS UMR5566/CNRS/CNES/IRD/UPS, France

8 <sup>3</sup> IWFM, BUET, Dhaka, Bangladesh

9 <sup>4</sup> Météo France, DIRAG, Martinique, France

10 <sup>5</sup> LIENSs UMR 7266 CNRS, University of La Rochelle, La Rochelle, France

11 \* Correspondence: ykrien@gmail.com; Tel.: +33 6 16 80 80 51

12

13 **Abstract:** Parametric cyclonic wind fields are widely used worldwide for insurance risk  
14 underwriting, coastal planning, or storm surge forecasts. They support high-stakes financial,  
15 development, and emergency decisions. Yet, there is still no consensus on the best parametric  
16 approach, or relevant guidance to choose among the great variety of published models. The aim of  
17 this paper is first and foremost to demonstrate that recent progresses on estimating extreme surface  
18 wind speeds from satellite remote sensing now makes it possible to select the best option with  
19 greater objectivity. In particular, we show that the Cyclone Global Navigation Satellite System  
20 (CYGNSS) mission of NASA is able to capture a substantial part of the tropical cyclones structure,  
21 and allows identifying systematic biases in a number of parametric models. Our results also  
22 suggest that none of the traditional empirical approaches can be considered as the best option in all  
23 cases. Rather, the choice of a parametric model depends on several criteria such as cyclone intensity  
24 and/or availability of wind radii information. The benefit of using satellite remote sensing data to  
25 better select a parametric model for a specific case study is tested here by simulating hurricane  
26 Maria (2017). The significant wave heights computed by a wave-current hydrodynamic coupled  
27 model are found to be in good accordance with the predictions given by the remote sensing data in  
28 terms of bias. The results and approach presented in this study should shed new light on how to  
29 handle parametric cyclonic wind models, and help the scientific community to conduct better  
30 wind, waves and surge analysis for tropical cyclones.

31 **Keywords:** Remote sensing; cyclones; parametric models; hurricanes; CYGNSS; ASCAT; storm  
32 surges; waves; winds

33

### 34 1. Introduction

35 Since the overview of Vickery et al. [1], numerical atmospheric models have been increasingly  
36 applied in storm surge prediction or coastal hazard assessment studies [2-5]. Nonetheless,  
37 parametric models deriving cyclonic wind fields from a few input parameters (pressure drop,  
38 maximum velocity, wind radii, location of the cyclone center, etc) are still widely used by the  
39 research and insurance communities, due to their simplicity, efficiency, and low-computational costs  
40 [6-12]. This is especially true for studies investigating storm surge hazards with statistical  
41 approaches, which require the construction of a large number of synthetic storms [13-16].

42 For a few decades (and still often today) the parametric surface winds were simply derived as the  
43 sum of an axisymmetric wind field and a uniform vector to mimic the asymmetry due to the storm  
44 translation speed. Vivid debates arose to determine the best way to estimate both components,

45 which is a particularly relevant issue since large discrepancies of the synthesized wind field occur  
46 depending on the chosen method [17]. This kind of approach where the tropical cyclone (TC) size is  
47 generally determined by a single parameter (the radius of maximum winds), presents several  
48 drawbacks. In particular, it generally does not satisfactorily represent the TC wind asymmetry,  
49 which can be due to many factors such as blocking action by a neighbor anticyclone, boundary layer  
50 friction, or terrestrial effects [18].

51 To date, the increasing availability of satellite remote sensing data makes it possible to better depict  
52 and forecast the wind structure of TCs and its variations with azimuth. Whether they are based on  
53 infrared imagery and data [19-21], scatterometry [22-23], X-band, C-band and L-band radiometry  
54 [24-29], or global navigation satellite system-reflectometry (GNSS-R) [30-32], all these data can  
55 provide information about the 34-kt, 50-kt, and/or 64-kt wind radii in each TC quadrant. These radii  
56 are now commonly reported in advisories issued by warning centers.

57 Yet, to our knowledge, only very few studies investigating TC winds, cyclonic-induced waves, or  
58 storm surges through parametric models account for all this information, whether for forecasts or  
59 hindcasts. Besides, it is striking to see that even now, there is neither consensus nor even real debate  
60 on the best gradient wind model, i.e. the parametric model that will represent with the greatest  
61 accuracy the increase and decay of wind speed as a function of distance to the TC center. A vivid  
62 example of this is the Holland [33] vortex. Although known to present significant drawbacks [34],  
63 this model is still widely used by the research and insurance communities all over the globe. Other  
64 commonly used parametric wind models (for which there is room for improvement) include for  
65 example Jelesnianski and Taylor [35], or Emanuel and Rotunno [36]. New models are proposed  
66 almost every year [18,37], but the published studies also generally suffer from one or several  
67 drawbacks, including:

- 68 • *a lack of information about the parameters considered.* For example, the empirical surface wind  
69 reduction factor (SWRF [38]) used for computations is rarely indicated, although it is thought to  
70 play a significant role in the estimated surface wind speeds [17].
- 71 • *comparisons/validations with a limited number of observed data.* In-situ observations of surface wind  
72 speed are relatively sparse for TCs, as they spend most of their lifetime over the oceans, where  
73 the density of buoys able to record extreme winds is relatively small. Besides, the wind  
74 recorded by meteorological stations is often biased because of terrestrial effects, which makes it  
75 difficult to compare observations with parametric values in a consistent way. Although these  
76 issues are offset to some extent in the North Atlantic and East Pacific thanks to aircraft  
77 reconnaissance, it remains a major problem in all oceanic basins.
- 78 • *comparisons/validations with a limited number of parametric wind models.* Except the work of Lin and  
79 Chavas [17], we are not aware of any study investigating parametric wind models over a wide  
80 range of parameters and methods. New proposed models are often compared to the Holland  
81 [33] or Jelesnianski and Taylor [35] approaches to assess their quality, and disregard more  
82 recent models such as Willoughby et al. [39] or Emanuel and Rotunno [36].
- 83 • *comparisons/validations with parametric models which do not include all the available information about  
84 the TC wind structure.* As noted before, very few studies take into account all the available  
85 information about wind structure, such as the 34-kt, 50-kt, and 64-kt wind radii for each  
86 quadrant. Most of the time, only the hurricane-force (i.e. 64kt) wind radii are used, which  
87 potentially results in errors far from the cyclone center.

88 Yet, indirect surface wind speed measurements using remote sensing data are now expected to be  
89 mature enough to help us overcome most of these limitations. The recent availability of data from  
90 CYGNSS (Cyclone Global Navigation Satellite System), a spatial mission dedicated to wind speeds  
91 retrieval near the eye of TCs, is a promising example.

92 The main objective of this paper is to investigate the benefits of using recent satellite remote sensing  
 93 data such as CYGNSS or ASCAT (Advanced Scatterometer) to help everyone selecting the most  
 94 suitable parametric model, depending on his own case study.

95 After a short description of data and wind models used in the present study (section 2), we compare  
 96 CYGNSS and ASCAT data with parametric models constrained by observations for 16 recent  
 97 hurricanes (section 3). The aim is to provide a first evaluation of the usefulness of these remote  
 98 sensing data as proxy for surface wind speeds. As we will show, these preliminary results suggest  
 99 that CYGNSS and ASCAT might indeed provide reliable estimates for extreme and moderate wind  
 100 speeds respectively. We then *hypothesize* that it is indeed the case, and check whether or not this  
 101 assumption leads to consistent results. To this aim, we first compute the biases given by several  
 102 parametric models to see if we can reproduce the findings of past studies (section 4). We then  
 103 perform numerical hindcasts of hurricane Maria (2017) using several parametric formulas, and  
 104 compare significant wave heights computed with real in-situ data to check, again, if the results are  
 105 consistent (section 5). We finally discuss the main results of the manuscript and give concluding  
 106 remarks (section 6).

107 **2. Data and Methods**

108 *2.1. Cyclone selection*

109 The Atlantic Ocean had a very active hurricane season in 2017, due to six major hurricanes and  
 110 two in category 5. Thanks to aircraft reconnaissance, large quantities of high-quality in-situ data  
 111 were collected and incorporated into models to better reproduce the hurricanes and their evolution  
 112 for a wide range of intensities and sizes. Besides, the CYGNSS mission of NASA (dedicated to  
 113 surface wind speed measurements in extreme conditions) was launched just in time to collect data  
 114 for this season. These conditions are ideal for revisiting the structure of TCs, and the ability of  
 115 parametric models to approximate it. In this study, we considered most of the hurricanes that  
 116 occurred both in Atlantic (ATL) and East Pacific (EP) during the 2017 season. In all, 16 events were  
 117 taken into account (Table 1).

118 **Table 1.** List and characteristics of the 16 hurricanes considered in this study. The minimum and  
 119 maximum radii at 34-kt, 50-kt, and 64-kts (R34, R50, and R64 respectively) are given in nautical miles  
 120 at the peak intensity. WS stands for wind speed.

Number	Name	Basin	Dates	TC Category (max WS)	Min/Max R34	Min/Max R50	Min/Max R64
1	Dora	EP	25/06 → 28/06	1 (80kt)	40/70	20/40	15/25
2	Eugene	EP	07/07 → 10/07	3 (100kt)	60/110	40/80	20/30
3	Franklin	ATL	07/08 → 10/08	1 (75kt)	60/130	30/50	NA/30
4	Gert	ATL	13/08 → 17/08	2 (90kt)	50/120	15/60	NA/30

5	Harvey	ATL	17/08 → 30/08	4 (115kt)	70/120	40/60	20/35
6	Hilary	EP	24/08 → 30/08	2 (90kt)	60/90	30/50	15/20
7	Irma	ATL	30/08 → 11/09	5 (160kt)	80/160	50/100	30/45
8	Irwin	EP	23/07 → 01/08	1 (80kt)	30/60	10/30	NA/15
9	Jose	ATL	05/09 → 22/09	4 (135kt)	50/120	30/50	20/30
10	Katia	ATL	06/09 → 09/09	2 (90kt)	60/60	20/40	15/20
11	Kenneth	EP	19/08 → 23/08	4 (115kt)	60/90	30/50	15/25
12	Lee	ATL	16/09 → 30/09	3 (100kt)	60/80	40/50	25/30
13	Maria	ATL	16/09 → 30/09	5 (150kt)	100/150	60/80	35/50
14	Max	EP	13/09 → 15/09	1 (70kt)	30/40	20/20	10/10
15	Norma	EP	14/09 → 19/09	1 (65kt)	70/80	30/50	NA/25
16	Otis	EP	16/09 → 19/09	3 (100kt)	40/60	20/40	10/20

121

122

123

124

125

For each of these events, we considered the following data provided by the NHC (National Hurricane Center) advisories: location of the cyclone center, minimum pressure, maximum wind speed, radii of the 34-, 50-, and 64-knot winds in the four quadrants at every 6 hours. Most of these data were calibrated using aircraft reconnaissance and are consequently expected to be reliable.

126

## 2.2. Remote sensing data

127

128

We also collected the full dataset distributed by the CYGNSS and ASCAT science team members for the 2017 hurricane season in Atlantic and East Pacific.

129 The CYGNSS mission [31] consists of a eight satellites-constellation in low-inclination circular  
130 orbit that receive direct and reflected GPS L1 (1.575 Ghz) signals to infer surface wind speeds and  
131 sea roughness, even for intense rainfalls typically observed during hurricanes. It allows for a good  
132 spatial and temporal coverage, with mean and median revisit times over the tropics of 7.2h and 2.8h  
133 respectively [32]. The 25km- resolution data considered here (v2.0) have been validated and  
134 calibrated using cyclones of the 2017 season, including most of the events considered in this study  
135 (Table 1). For the time being, the overall root mean square (RMS) error in the CYGNSS retrievals is  
136 about 1.4m/s and 17% for wind speeds lower and larger than 20 m/s respectively [40]. According to  
137 the CYGNSS team (personal communication), the bias explains approximately half of the high wind  
138 RMS (about 8.5%), the other half being random scatter. Generally speaking, we can thus expect  
139 maximum biases of a few meters per second, even for high wind speeds.

140

141 We tested here several Level 2-wind speed products:

142

- 143 • The "wind speed" (*ws*) product is derived from the best fit to both the normalized bistatic radar  
144 cross-section (NBRCS) and leading edge slope (LES) of the integrated delay waveform given by  
145 the delay-Doppler maps (DDM [41]), using a fully developed seas geophysical model function  
146 (GMF);
- 147 • The "yslf\_les\_wind\_speed" (*les*) wind product is derived from only the LES of the DDM, using a  
148 young seas / limited-fetch GMF;
- 149 • The "yslf\_nbrcs\_wind\_speed" (*nbrc*) product is derived from only the NBRCS, using the young  
150 seas / limited-fetch GMF.

151

152 ASCAT [22,42] consists of C-band scatterometers mounted on the satellites MetOp-A and  
153 MetOp-B, that were launched in 2006 and 2012 respectively. The emitting antennas transmit pulses  
154 at 5.255 GHz and extend on either side of the instrument, which results in a double 500km-wide  
155 swath of observations. These scatterometers are found to give reliable estimations of wind speeds up  
156 to at least 34-kt. However, they lose sensitivity in extreme conditions and are often plagued by rain  
157 contamination. We use here the 25km-resolution coastal product, which give more wind data close  
158 to the coast [43].

159

### 2.3. Parametric wind models

160

161 For a given cyclone and parametric gradient wind profile, we estimated the surface wind speed  
162 associated to each CYGNSS and ASCAT data point according to the following main steps:

163

164 1- From the NHC advisories, we estimated the surface background wind relative to the cyclone  
165 translation velocity at the time of acquisition of the considered CYGNSS/ASCAT data point.  
166 Following the approach of Lin and Chavas [17], we assumed that this wind is decelerated by a factor  
167  $\alpha=0.56$  and rotated counter-clockwise by an angle  $\beta=19.2^\circ$  from the free tropospheric wind.

168

169 2-We removed the translational portion of the wind speed from the maximum observed wind  
170 velocity and the 34-, 50-, and 64kt winds.

171

172 3-We converted surface velocities to velocities on top of the atmospheric boundary layer by  
173 applying an empirical surface wind reduction factor SWRF [38]. In the following sections, we  
174 specified SWRF=0.9. Other values were tested, but for the sake of simplicity results are not presented  
175 here (they add very little to the conclusions of this paper).

176

177 4-We estimated the maximum wind radii for the four quadrants, using the chosen parametric  
178 gradient wind profile, and the available wind radii information. For each quadrant, up to three radii  
179 of maximum wind are thus obtained: one from the 64-kt wind radius ( $R_{m64}$ ), another from the 50-kt  
wind radius ( $R_{m50}$ ), and a last one from the 34-kt wind radius ( $R_{m34}$ ).

180

181 5-Depending on the available wind radii information considered, we computed  $R_{m64}$ ,  $R_{m34}$  or all  
 182 the radii of maximum winds ( $R_{m64}$ ,  $R_{m50}$ , and  $R_{m34}$ ) for the data point azimuth, using a spline  
 183 interpolation.

184

185 6-We computed the wind speed values at the CYGNSS/ASCAT data point obtained using the  
 186 chosen parametric gradient wind profile and the radii of maximum winds considered ( $R_{m64}$ ,  $R_{m34}$ , or  
 187 all three of them).

188 7-We assessed the wind speed at the CYGNSS/ASCAT data point, using a weighted average of  
 189 the wind speeds obtained in the previous step. We followed the procedure proposed by Hu et al.  
 190 [44], which ensures that all the wind radii information is satisfied.

191

192 8-We obtained the surface wind speed by multiplying the result by SWRF.

193

194 9-The wind speed obtained in the previous step was combined with the surface background  
 195 wind computed in step 1 to get the final parametric wind speed at the CYGNSS/ASCAT data point  
 196 considered.

197

198 This procedure is repeated for all the storms, gradient wind profiles, and CYGNSS/ASCAT  
 199 Level 2-data points within a distance of 200km from the cyclone center. The parametric models  
 200 considered here are given in Table 2.

201

202 **Table 2.** Parametric wind models considered in this study. For all of them, an empirical surface wind  
 203 reduction factor [38] SWRF=0.9 was prescribed. Comparisons are only made for data within a  
 204 distance of 200km from the cyclone center. The translation vector is reduced by a factor  $\alpha=0.56$  and  
 205 rotated counter-clockwise by an angle  $\beta=19.2^\circ$ , according to the findings of Lin and Chavas [17].  
 206 Here,  $V_m$  and  $R_m$  are the maximum wind speed and the radius of maximum winds.  $r$  refers to the  
 207 distance to the TC center, and  $f$  to the coriolis coefficient.

Name	Main reference	Formula
E11	<i>Emanuel and Rotunno [36]</i>	$V(r) = \frac{2r(R_m V_m + 0.5f R_m^2)}{R_m^2 + r^2} - \frac{fr}{2}$
E04	<i>Emanuel [45]</i>	$V(r) = V_m \frac{R_{0-r}}{R_0 - R_m} \left( \frac{r}{R_m} \right)^m \left( \frac{(1+b)(n+m)}{n+m \left( \frac{r}{R_m} \right)^{2(n+m)}} + \frac{b(1+2m)}{1+2m \left( \frac{r}{R_m} \right)^{2m+1}} \right)^{0.5}$ with $b=0.25$ , $m=1.6$ , $n=0.9$ , $R_0=420\text{km}$
J92	<i>Jelesnianski et al [46]</i>	$V(r) = \frac{2rR_m V_m}{R_m^2 + r^2}$
H80	<i>Holland [33]</i>	$V(r) = \sqrt{\left( \frac{R_m}{r} \right)^B B \Delta P \exp \left( - \left( \frac{R_m}{r} \right)^B \right)} + \frac{r^2 f^2}{4} - \frac{fr}{2}$

		with $B = \frac{V_m^2 e \rho + f V_m R_m e \rho}{\Delta P}$ , $\rho = 1.15$ , $e = \exp(1)$
H80c	<i>Holland [33] with cyclostrophic approximation</i>	$V(r) = \sqrt{\left(\frac{R_m}{r}\right)^B B \Delta P \exp\left(-\left(\frac{R_m}{r}\right)^B\right)}$ with $B = \frac{V_m^2 e \rho}{\Delta P}$ , $\rho = 1.15$ , $e = \exp(1)$
M16	<i>Murty et al. [37]</i>	$V(r) = V_m \left(\frac{2rR_m}{(R_m^2+r^2)}\right)^n$ with $n = 3/5$
W06	<i>Willoughby et al. [39]</i>	For $0 \leq r \leq R_m$ : $V(r) = V_m \left(\frac{r}{R_m}\right)^n$ with $n = 0.79$ For $r \geq R_m$ : $V(r) = V_m \exp\left(-\frac{r-R_m}{X}\right)$ with $X = 243\text{km}$

208

209 **3. Comparison of CYGNSS and ASCAT data**

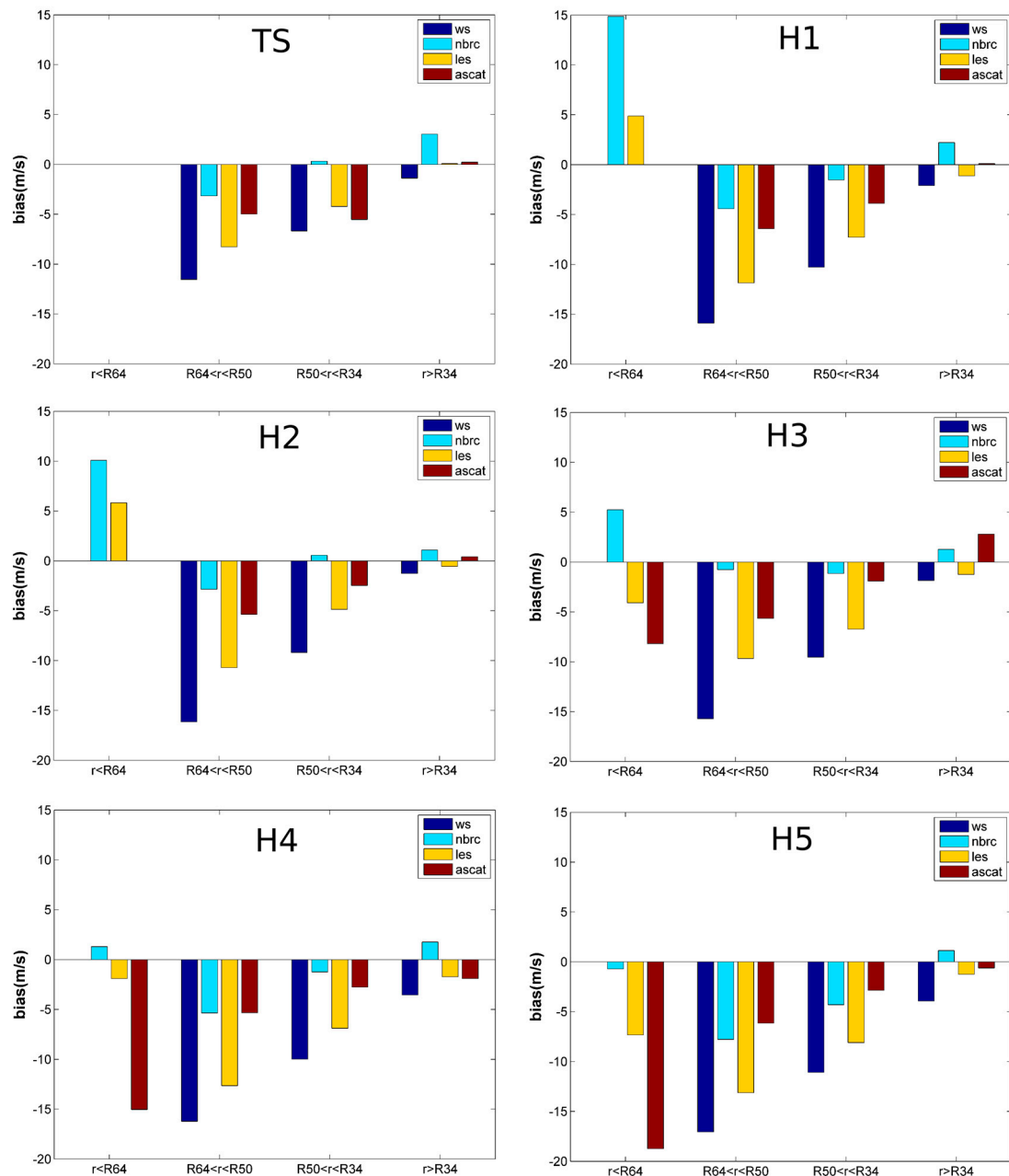
210

211 To get a preliminary idea of the usefulness of CYGNSS and ASCAT data as proxy for surface  
 212 wind speeds, we computed the biases between these data and the mean (i.e. averaged over all  
 213 empirical models) parametric winds for different cyclone categories and distances to the center  
 214 (Figure 1). Computations were performed only when more than 30 data points were available for a  
 215 given intensity/distance class. In practice, the comparison was possible for almost all cases, as  
 216 hundreds or even thousands of space-borne observations were available for each class. Parametric  
 217 models have been constrained by all the information provided by the NHC in the advisories, to  
 218 ensure that they give the best approximation possible to real winds. In classes for which the biases  
 219 are large, remote sensing data are not consistent with the mean parametric winds. We choose not to  
 220 investigate further these data in the following sections, even if there is no evidence that the error is  
 221 due to remote sensing rather than parametric models. On the contrary, small biases (in absolute  
 222 terms) suggest that remote sensing data and parametric winds are consistent, so that they both give  
 223 satisfactory results *a priori*. In the following, we will make the assumption that these  
 224 CYGNSS/ASCAT data are indeed good proxies, and check whether or not this hypothesis leads to  
 225 consistent results.

226

227

228



229  
230 **Figure 1.** Bias between the remote sensing data and the parametric winds averaged over all  
231 empirical models (negative/positive values indicate that remote sensing data are  
232 negatively/positively biased compared to the mean parametric winds) . Different categories of  
233 distance to the cyclone center (r) and cyclone intensities are considered. TS stands for tropical  
234 storms, H1, H2, H3, H4, and H5 to the cyclone category (1, 2, 3, 4, and 5 respectively). R34,  
235 R50, and R64 are the radii for the 34-kt, 50-kt, and 64-kt winds. *ws*, *nbrc*, and *les* are three  
236 different CYGNSS products (see section 2).

237  
238 Regarding ASCAT data, Figure 1 shows that the bias is low (less than about 2-3m/s in absolute  
239 value) for radius larger than R34, but becomes increasingly negative with cyclone category and  
240 decreasing distance to the cyclone center, up to almost -20m/s. These results suggest that ASCAT  
241 data are a good proxy for wind speeds lower than 34-kt, but that they underestimate extreme winds.  
242 This conclusion is consistent with previous published papers [47].

243 The "wind speed" (*ws*) product is found to give systematically more negative biases than  
244 ASCAT, and thus probably often underestimates the velocities (Figure 1). However, the absolute  
245 value of bias remains relatively low for radius larger than R34, which suggests that this product

246 might still be a good proxy for moderate and (potentially even more) low wind speeds. As this  
247 product was developed for fully developed seas, these results were also expected.

248 Wind speeds derived from only the LES of the DDM ("les" in Figure 1) display, again, negative  
249 biases for  $r > R64$ . However, those remain smaller in absolute value compared to "ws", which makes  
250 sense since this product has been derived using a young seas / limited-fetch GMF that is expected to  
251 be more suitable for our test cases. Considering the potential errors on parametric models, it could  
252 be a proxy as good as ASCAT for radius larger than R34. Above all, this product shows significantly  
253 reduced biases for  $r < R64$ . This suggests that it yields better estimates of surface wind speeds than  
254 ASCAT close to the eyewall.

255 The wind speeds derived from only the NBRCS ("nbrc" in Figure 1) outperform the other  
256 products in most cases for radius lower than R34, with bias generally lower than 5m/s in absolute  
257 value. The main exception is the wind for radius lower than R64 for minor cyclones (category 1 or 2),  
258 where the bias reaches 10 to 15m/s. One plausible explanation is that the resolution of CYGNSS  
259 (25km) is too low to capture the surface wind speeds in these area, especially for weak cyclones  
260 where the 64kt radii are very close to the eyewall, i.e. to places where wind speeds vary quickly as a  
261 function of distance to the center. This problem is presumably less severe for major cyclones  
262 (category 3 or more) because of a larger extent of hurricane-force winds (Table 1).

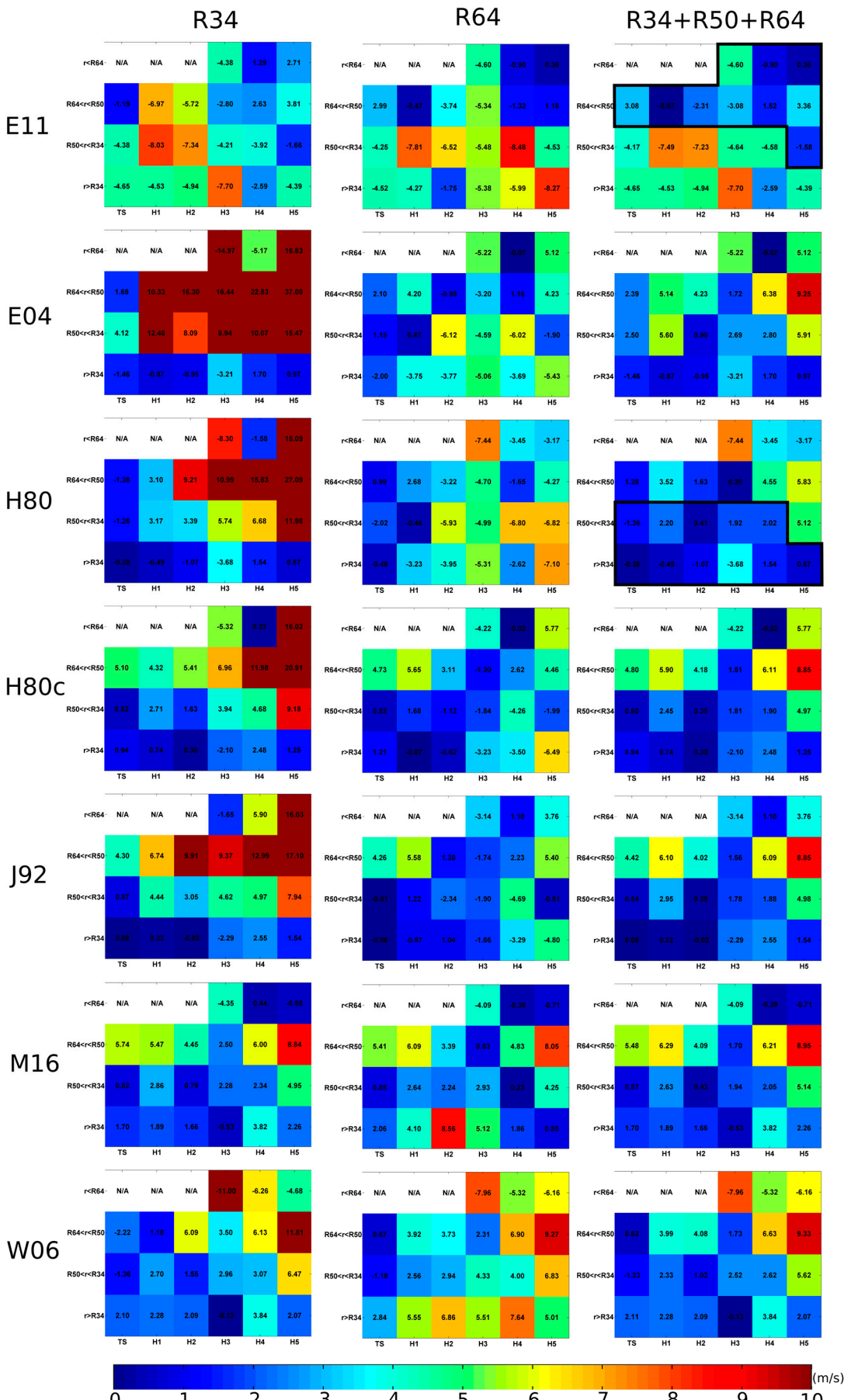
263  
264 Based on all these findings, we will *hypothesize* in the following section that the ASCAT and  
265 CYGNSS/NBRC products are the best surface wind speeds proxy for  $r > R34$  and  $r < R34$  respectively.  
266 However, we will not consider radii lower than R64 for weak (category 1-2) cyclones, as Figure 1  
267 also suggest that none of the space-borne products tested here is reliable in these conditions.

268  
269 We will check in sections 4 and 5 whether these preliminary results and assumptions give  
270 results consistent with previous work and in-situ data, to confirm or invalidate them *a posteriori*.

#### 271 4. Performance of parametric wind models

272 Using the assumption made in the previous section, we computed the bias of the various  
273 parametric models as a function of storm intensity, distance to the cyclone center, and calibration  
274 method (using only radii at 34kt, only radii at 64kt, and all radii information for the left, middle and  
275 right panels respectively in Figure 2). The color bar shows the absolute value of bias. Blue colors  
276 correspond to small biases (in absolute value), and thus suggest that the parametric model should  
277 work well for the intensity/distance class considered. Conversely, red colors indicate that the model  
278 is expected to perform poorly. The aim is to see whether the assumption on which this figure is  
279 based ("ASCAT and CYGNSS/NBRC are good wind speeds proxy for  $r > R34$  and  $r < R34$   
280 respectively") gives consistent results or not.

281



283 **Figure 2.** Diagrams displaying the bias between various parametric models and the surface  
284 wind speeds estimated by CYGNSS/ASCAT data for all the events considered here, as a function of  
285 storm intensity and distance to the cyclone center (x- and y-axis respectively for each diagram), as  
286 well as calibration method (using only radii at 34kt, only radii at 64kt, and all radii information for  
287 the left, middle and right panels respectively). The color bar (the same for all diagrams) shows the  
288 absolute value bias. The values are displayed for each category/distance cell. The black contours  
289 indicate the category/distance classes for which we consider E11 and H80 models in section 5 (model  
290 E11H80).

291 First of all, it appears that the bias is significantly reduced in almost all cases for  $r < R64$  and  $r > R34$   
292 when constraining the parametric models by R64 and R34 respectively. This suggests that not only  
293 the "mean" parametric wind values computed in section 3 are consistent with the CYGNSS/ASCAT  
294 data for these classes, but also most of the parametric models taken individually, as long as they are  
295 constrained by the 64-kt and 34-kt wind radii given by the NHC. This finding gives additional credit  
296 to the assumption we made in section 3. It may, however, be observed that biases are not always so  
297 much reduced (and can even be increased) when constraining the parametric models by R50 for very  
298 intense (category >3) cyclones. This issue appears also in Figure 1, where strangely the absolute bias  
299 of CYGNSS is larger for  $R64 < r < R50$  than for  $r < R64$ . There could be several explanations to this fact:  
300 an issue with the calibration of CYGNSS data for these conditions of course, but also a problem with  
301 the parametric models for extreme events in the "transition zone" (the area between the inner  
302 core/outer region). The latter cannot be dismissed, as most parametric models were built by focusing  
303 mainly on the inner and/or outer regions (e.g. [39]), whereas much less attention was paid to the  
304 transition zone between extreme and moderate winds. We will return to this point later on.

305 The results are also found to be consistent with most of the previous works. For instance:

- 306 • The inner region solution of Emanuel and Rotunno [36], E11, generally gives the smaller bias  
307 (hence the best results) close to the storm center (typically, for  $r < R50$ ), especially for intense and  
308 well defined cyclones. It is also found to underestimate significantly the wind speeds far from  
309 the center as found in Lin and Chavas [17], even when prescribing the radii at 34-kt. E04  
310 performs much better for the outer region, but poorly near the center. E11 and E04 can thus be  
311 merged to develop a complete TC radial wind structure as proposed by Chavas et al. [48];
- 312 • When solely constrained by radii close to the cyclone center (here R64), the Holland profile  
313 (H80) tends to underestimate the winds in the outer region, as noted by Willoughby and Rahn  
314 [34]. It can also lead to broad wind maximum, and thus wind overestimations at several dozens  
315 of kilometers from the center for extreme cyclones (for  $R64 < r < R50$  for example), as can be seen  
316 in the right and left panels notably. These findings, which are in accordance with the results of  
317 Willoughby and Rahn [34], confirm that the issue we identified earlier with the 50-kt wind radii  
318 could be partly due to flaws in parametric models such as H80 in the "transition zone".
- 319 • J92 tends to overestimate the wind speeds by a few m/s, as suggested by Lin and Chavas [17];
- 320 • The results are generally much better when considering a family of profiles with two  
321 characteristic lengths, as proposed by Willoughby et al [39]. For example, as stated above, the  
322 performance of the Holland model H80 is significantly increased when both radii at 34-kt and  
323 64-kt are prescribed;
- 324 • Models such as W06 or M16 (which decay exponentially or as a power-law outside the eye)  
325 perform well in the outer region when the 34-kt radii are prescribed properly, which is  
326 consistent with the findings of Willoughby et al. [39] and Murty et al. [37].

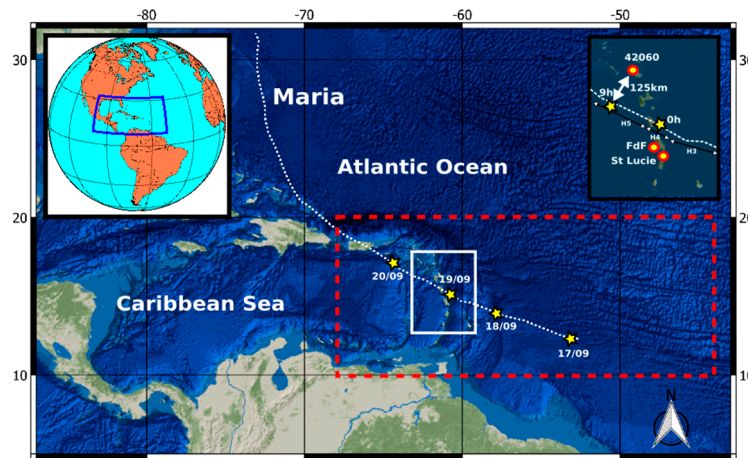
327 The consistency of these results increases the confidence in our assumption that the ASCAT and  
328 CYGNSS/NBRC products are relatively good proxies for surface wind speeds, for  $r > R34$  and  $r < R34$   
329 respectively (with the exception of the inner region for weak cyclones). To further build the  
330 confidence in this hypothesis, we also performed numerical hindcasts of hurricane Maria (2017), and  
331 compared computed significant wave heights with real in-situ data (section 5). The aim was also to

332 investigate the potential of results such as those presented in Figure 2 to choose one parametric  
 333 model rather than another, depending on the case study.

334 **5. Comparison with in-situ data**

335 Hurricane Maria was the deadliest storm of the 2017 Atlantic season. Recorded as a category 5  
 336 event, it caused catastrophic damages in Dominica and Puerto Rico, as well as widespread flooding  
 337 and crop destructions in Guadeloupe. We tested here the ability of several parametric models to  
 338 properly represent the wind pattern evolution during Maria by comparing the significant wave  
 339 heights observed at buoys in the Lesser Antilles with those computed using a wave-current coupled  
 340 model forced by a sub-set of the various parametric winds considered in the previous section. The  
 341 model is based on the code SCHISM-WWM [49]. The computational domain is represented in Figure  
 342 3. Resolution spans from 10km far from the region of interest (where the bathymetry is derived from  
 343 GEBCO), up to about 100m in Guadeloupe and Martinique where we have the best bathymetric data  
 344 (ship-based soundings from the SHOM, the French Naval Hydrographic and Oceanographic  
 345 Department). The model is forced by:

- 346 • astronomic tidal potential over the whole domain (12 constituents);
- 347 • 26 tidal harmonic constituents at the open boundaries, provided by the global FES2012 model  
 348 [50] ;
- 349 • parametric pressure fields [33];
- 350 • parametric winds blended with CFSR (Climate Forecast System Reanalysis [51]) wind data. The  
 351 parametric winds are prescribed for radii less than  $R_{34}$ , whereas CFSR data are imposed for  $r >$   
 352  $1.5 R_{34}$ . In between, a smooth transition is ensured using a weighing coefficient varying with  
 353 the radius  $r$ .



355  
 356 **Figure 3.** Study area. The computational domain is depicted with the dashed red contour. The  
 357 dashed white line represents the track of hurricane Maria. The location of the buoys used for  
 358 comparison is given in the upper-right corner box.

359  
 360 We considered here five parametric models:

- 361 • E11 and H80, constrained using the 64-kt wind radii only (E11(R64) and H80(R64) in Figure 4);
- 362 • E11 and H80, constrained using all the wind radii information (E11(All) and H80(All) in Figure  
 363 4);
- 364 • E11H80, for which we chose to blend the wind speeds inferred from E11 for the inner core area  
 365 with those given by H80 for the outer region (see the black contours in Figure 2)

366  
 367 E11H80 was chosen to test whether results such as those presented in Figure 2 could be of benefit to  
 368 build a better parametric model for the cyclone considered, using a combination of models that is  
 369 expected to reduce the biases. We strongly insist on the fact that the new model tested here (E11H80)

370 is just an example. In no way we consider this model as the best option. E11 combined with W06 or  
 371 E04 could be also tested for instance.

372

373 The reader is referred to Krien et al [9] for greater details about the model and the numerical  
 374 strategy. Here, we compared the significant wave heights (Hs) computed by the model with the Hs  
 375 recorded by three buoys located in the Lesser Antilles (Figure 3): Fort de France (FdF) and Sainte  
 376 Lucie, owned by Meteo France, as well as 42060, maintained by the National Data Buoy Center  
 377 (NDBC). The latter went adrift during the peak of Maria, hence the decrease of Hs was unfortunately  
 378 not captured.

379

380 **Table 3.** Bias, root mean square error (RMS) and normalized RMS (NRMS) obtained when  
 381 comparing numerical simulations with in-situ significant wave heights.

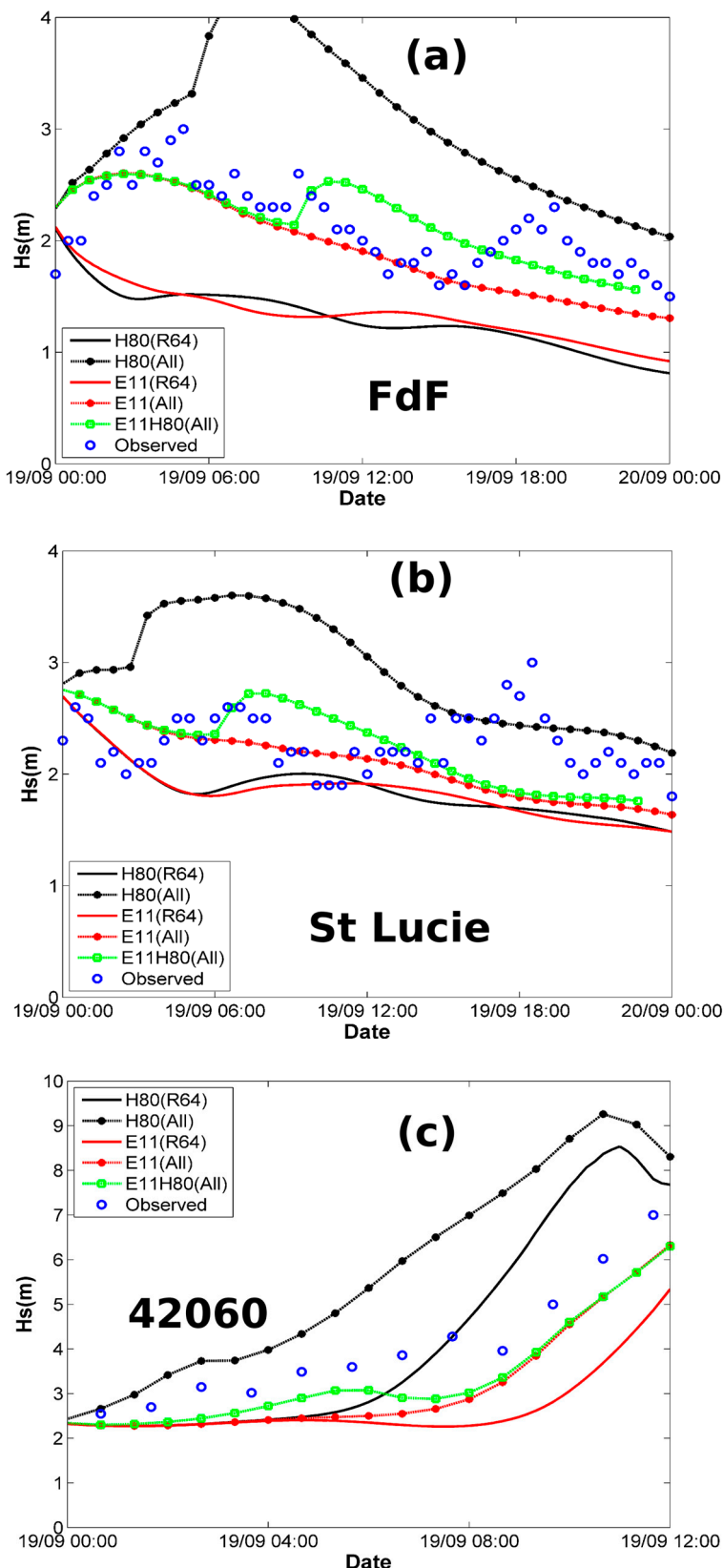
		42060	Fort de France	St Lucie
H80 (R64)	Bias	0.1m	-0.85m	-0.43m
	RMS	1.2m	0.9m	0.55m
	NRMS	27.1%	41.8%	24%
H80 (All)	Bias	1.5m	0.9m	0.64m
	RMS	2m	1.06m	0.84m
	NRMS	46%	49.3%	36.6%
E11 (R64)	Bias	-1.4m	-0.8m	-0.44m
	RMS	1.5m	0.87m	0.56m
	NRMS	35%	40.3%	24.5%
E11 (All)	Bias	-0.9m	-0.21m	-0.19m
	RMS	0.9m	0.34m	0.43m
	NRMS	21.3%	15.8%	18.7%
E11H80 (All)	Bias	-0.7m	0.01m	-0.04m
	RMS	0.7m	0.31m	0.44m
	NRMS	17.4%	14.5%	19.2%

382 Results (Table3, Figure 4) show that:

383 • H80 and E11 constrained only by the 64-kt wind radii (R64) give the worst results, with Hs  
 384 generally significantly underestimated, and NRMS ranging between 20% and 50% (Table 3).

385 • Trying to improve these models by constraining all the 34-kt, 50-kt, and 64-kt wind radii (All)  
386 results in much better performances for E11, with reduced bias and NRMS (15 to 22%  
387 approximately). This suggests that E11 satisfactorily represents the TC structure, at least as long  
388 as the hurricane (here in category 4-5) remains relatively close to the buoys. It tends to  
389 underestimate Hs (in Sainte Lucie for example) when the storm moves further away.  
390 • On the contrary, the H80 model strongly overestimates Hs when Maria is the closest to the  
391 storm, at a distance of about 120-200km (which corresponds roughly to the radii at 50-kt). This  
392 is also consistent with the results of Figure 2, and confirms, again, that the relatively significant  
393 biases obtained in Figure 1 for extreme cyclones and  $R_{64} < r < R_{50}$  might be partly explained by  
394 flaws in parametric models such as H80 rather than errors in CYGNSS wind speeds. The  
395 prediction is better when Maria moves further away, which was also expected.  
396 • The best results are obtained here for the model E11H80. The bias is found to be considerably  
397 reduced compared to E11constrained with all wind radii.  
398

399 These results are all consistent with those presented in Figure 2 (keeping in mind that Maria is  
400 here a category 4-5 hurricane, and that it passes relatively close to the buoys, see Figure 3). Hence  
401 they also support our assumption that the ASCAT and CYGNSS/NBRC products are relatively good  
402 proxies for surface wind speeds, for  $r > R_{34}$  and  $r < R_{34}$  respectively (with the exception of the inner  
403 region for weak cyclones).  
404  
405  
406



407  
408  
409  
410  
411  
412  
413

**Figure 4**- Significant wave height time series for different parametric models. "R64" denotes a model constrained only by the 64-kt wind radii. "ALL" indicates a model constrained with all the available information (34-kt, 50-kt, and 64-kt wind radii). E11H80 corresponds to a blend of the model E11 (for the inner core region) and H80 (for the outer region). Results for Fort-de-France, Sainte-Lucie, and the 42060 station are displayed in (a), (b), and (c) respectively.

414 **6. Conclusions**

415 Taking advantage of an extremely active 2017 hurricane season in the tropical Atlantic Ocean and the  
416 Eastern Pacific, we investigated the potential of using recent satellite remote sensing data such as CYGNSS and  
417 ASCAT to identify the advantages and drawbacks of several parametric wind models used for storm surge  
418 hazard assessment or prediction of cyclonic waves.

419 Under the assumption that ASCAT and CYGNSS/NBRC products can be considered as good proxies for surface  
420 wind speeds for the outer and inner regions respectively (with an exception for the core of weak cyclones), we  
421 were able to confirm the findings of a number of previous studies (e.g. Willoughby et al. [39], Lin and Chavas  
422 [17] or Chavas et al. [48]). Using a wave-current coupled numerical model, we also showed that remote sensing  
423 data such as CYGNSS/ASCAT are probably sufficiently accurate to be used to better select a suitable parametric  
424 model, depending on the case study considered. The choice will depend on several criteria such as cyclone  
425 intensity and/or availability of wind radii information. Indeed, our results suggest that none of the traditional  
426 empirical approaches can be considered as the best option in all cases.

427 We strongly insist on the fact that our aim here is not to encourage using or discarding a specific parametric  
428 model, and even less to propose a new one. First, because we did not test all the published models. Second,  
429 because each author uses a specific combination of parameters and approach to mimic the wind field, so that it  
430 would be presumptuous to draw definitive conclusions. Besides, there are still errors on remote sensing data, so  
431 that differences of 2-3m/s in terms of bias are probably not really significant.

432 The main finding of this paper is thus the following: satellite remote sensing is now mature enough to provide  
433 relevant information about the performance of parametric cyclonic wind models, even if further work is  
434 needed, especially to access to the full structure of TCs close to the eyewall. We focused here mainly on the  
435 CYGNSS mission, but there is little doubt that other type of data can also be valuable. Remote sensing has now  
436 become a powerful tool that should be used to validate or improve existing parametric approaches, in order to  
437 conduct better wind, waves, and surge analysis for TCs.

438 It is noteworthy to conclude by mentioning that even with the improved model tested here for Maria (see  
439 section 5), the NRMS remains relatively high (15-20%). Indeed, the temporal resolution (6-hours) is not  
440 sufficient to allow parametric models to reproduce the short-term variations of track, translation speed, or wind  
441 asymmetry. This stresses the need for higher temporal sampling of data (location of the cyclone center,  
442 maximum wind speed, wind radii, etc), and greater efforts to improve the efficiency of numerical atmospheric  
443 models.

444 **Acknowledgments:** This study was founded by the ERDF/C3AF project as well as the IRD. Our warm thanks to  
445 the CYGNSS and ASCAT science team members for their work. ASCAT and CYGNSS data were provided by  
446 the KNMI and PODAAC data center respectively. Data at Fort-de-France and Sainte-Lucie were made available  
447 by the CEREMA (CANDHIS database). The significant wave heights at station 42060 were provided by NDBC.

448 **Author Contributions:** Yann Krien conceived the idea and wrote most of the paper; Gaël Arnaud, Raphaël  
449 Cécé and Jamal Khan contributed to the development of the analysis tools; Gaël Arnaud, Ali Bel Madani and  
450 A.K.M.S. Islam arranged the figures and corrected a number of errors in the first version of the manuscript.  
451 Didier Bernard, Philippe Palany and Narcisse Zahibo prepared the project C3AF which funded about 66% of  
452 the work presented here. Fabien Durand, Laurent Testut and A.K.M.S. Islam played a major role for obtaining  
453 the IRD grant (about one third of total fundings). The manuscript also greatly benefited from their  
454 proofreading and suggestions.

455 **Conflicts of Interest:** The authors declare no conflict of interest.

456 **References**

1. Vickery, P. J., Masters, F.J., Powell, M.D., Wadhena, D. Hurricane hazard modeling: The past, present, and future, *J. Wind Eng. Ind. Aerodyn.* **2009**, *97*, 392–405, doi:10.1016/j.jweia.2009.05.005.
2. Lin, N., Smith, J.A., Villarini, G., Marchok, T.P., Baeck, M.L. Modeling extreme rainfall, winds, and surge from Hurricane Isabel (2003), *Weather Forecast.* **2010**, *25*, 1342–1361, doi:10.1175/2010WAF2222349.1.
3. Hsiao, L. F., Chen, D.S., Kuo, Y.H., Guo, Y.R., Yeh, T.C., Hong, J.S., Fong, C.T., Lee, C.S. Application of WRF 3DVAR to operational typhoon prediction in Taiwan: Impact of outer loop and partial cycling approaches. *Wea. Forecasting* **2012**, *27*, 1249–1263, doi:10.1175/WAF-D-11-00131.1.
4. Powers, J., Klemp, J., Skamarock, W., Davis, C., Dudhia, J., Gill, D., Coen, J., Gochis, D., Ahmadov, R., Peckham, S., Grell, G., Michalakes, J., Trahan, S., Benjamin, S., Alexander, C., DiMego, G., Wang, W.,

466 Schwartz, C., Romine, G., Liu, Z., Snyder, C., Chen, F., Barlage, M., Yu, W., Duda, M. The weather research  
467 and forecasting (WRF) model: overview, system efforts, and future directions. *Bull. Am. Meteorol. Soc.* **2017**,  
468 <http://dx.doi.org/10.1175/BAMS-D-15-00308.1>

469 5. Lakshmi, D., Murty, P.L.N., Bhaskaran, P.K., Sahoo, B., Srinivasa Kumar, T., Shenoi, S.S.C., Srikanth, A.S.  
470 Performance of WRF-ARW winds on computed storm surge using hydrodynamic model for Phailin and  
471 Hudhud cyclones. *Ocean. Eng.* **2017**, 131, 135–148.

472 6. Mattocks C., Forbes C. A real-time, event-triggered storm surge forecasting system for the state of North  
473 Carolina. *Ocean. Model.* **2008**, 25:95–119.

474 7. Lin, N., Emanuel, K.A. Grey swan tropical cyclones. *Nat. Climate Change* **2016**, 6, 106–111,  
475 doi:10.1038/nclimate2777.

476 8. Orton, P. M., Hall, T.M., Talke, S.A., Blumberg, A.F., Georgas, N., Vinogradov, S. A validated  
477 tropical-extratropical flood hazard assessment for New York harbor. *J. Geophys. Res. Oceans* **2016**, 121,  
478 8904–8929, <https://doi.org/10.1002/2016JC011679>.

479 9. Krien, Y., Testut, L., Durand, F., Mayet, C., Islam A.K.M.S., Tazkia, A.R., Becker, M., Calmant, S., Papa, F.,  
480 Ballu, V., Shum, C.K., Khan, Z.H. Towards improved storm surge models in the northern Bay of Bengal.  
481 *Continental Shelf Research* **2017**, 135, 58–73.

482 10. Shao, Z., Liang, B., Li, H., Wu, G., Wu, Z. Blended wind fields for wave modeling of tropical cyclones in  
483 the South China Sea and East China Sea. *Applied Ocean Research* **2018**, 71, 20–33.

484 11. Feng, X., Li, M., Yin, B., Yang, D., Yang, H. Study of storm surge trends in typhoon-prone coastal areas  
485 based on observations and surge-wave coupled simulations. *Int. J. Appl. Earth Obs. Geoinf.* **2018**,  
486 <https://doi.org/10.1016/j.jag.2018.01.006>.

487 12. Tan, C., Fang, W. Mapping the Wind Hazard of Global Tropical Cyclones with Parametric Wind Field  
488 Models by Considering the Effect of Local Factors. *Int. J. Disaster Risk Sci.* **2018**,  
489 <https://doi.org/10.1007/s13753-018-0161-1>.

490 13. Niedoroda, A. W., Resio, D. T., Toro, G. R., Divoky, D., Das, H. S., and Reed, C. W. Analysis of the coastal  
491 Mississippi storm surge hazard, *Ocean Eng.* **2010**, 37, 82–90.

492 14. Haigh, I. D., MacPherson, L. R., Mason, M. S., Wijeratne, E. M. S., Pattiaratchi, C. B., Crompton, R. P., and  
493 George, S. Estimating present day extreme water level exceedance probabilities around the coastline of  
494 Australia: tropical cyclone-induced storm surges, *Clim. Dynam.* **2014**, 42, 139–157.

495 15. Krien, Y., Dudon, B., Roger, J., Zahibo, N. Probabilistic hurricane-induced storm surge hazard assessment  
496 in Guadeloupe, Lesser Antilles. *Nat. Haz. Earth Syst. Sci.* **2015**, 15, 1711–1720.

497 16. Krien, Y., Dudon, B., Roger, J., Arnaud, G., Zahibo, N. Assessing storm surge hazard and impact of sea  
498 level rise in Lesser Antilles—Case study of Martinique. *Nat. Haz. Earth Syst. Sci.* **2017**, 17, 1559–1571.

499 17. Lin, N., Chavas, D. On hurricane parametric wind and applications in storm surge modeling. *J. Geophys.*  
500 *Res.* **2012**, 117, D09120. <http://dx.doi.org/10.1029/2011JD017126>.

501 18. Olfateh, M., Callaghan, D.P., Nielsen, P., Baldock, T.E. Tropical cyclone wind field  
502 asymmetry—development and evaluation of a new parametric model, *J. Geophys. Res. Oceans* **2017**, 122,  
503 458–469.

504 19. Knaff, J.A., S.P. Longmore, R.T. DeMaria, Molenar, D.A. Improved Tropical-Cyclone Flight-Level Wind  
505 Estimates Using Routine Infrared Satellite Reconnaissance. *J. Appl. Meteor. Climatol.* **2015**, 54, 463–478.

506 20. Dolling, K., E. Ritchie, Tyo, J. The Use of the Deviation Angle Variance Technique on Geostationary  
507 Satellite Imagery to Estimate Tropical Cyclone Size Parameters. *Wea. Forecasting* **2016**, 31, 1625–1642, doi:  
508 10.1175/WAF-D-16-0056.1.

509 21. Mueller, K. J., DeMaria, M., Knaff, J.A., Kossin, J.P., Vonder Haar, T.H. Objective estimation of tropical  
510 cyclone wind structure from infrared satellite data. *Wea. Forecasting* **2006**, 21, 990–1005,  
511 doi:10.1175/WAF955.1.

512 22. Figa-Saldana, J., Wilson, J.J.W., Attema, E., Gelsthorpe, R., Drinkwater, M.R., Stoffelen, A. The advanced  
513 scatterometer (ASCAT) on the meteorological operational (MetOp) platform: A follow on for European  
514 wind scatterometers. *Canadian Journal of Remote Sensing* **2002**, 28, 404–412.

515 23. Madsen, N. M., Long, D.G. Calibration and Validation of the RapidScat Scatterometer Using Tropical  
516 Rainforests. *IEEE Trans. Geosci. Remote Sens.* **2016**, 54, 2846–2854.

517 24. Meissner, T., Wentz, F.J. Wind vector retrievals under rain with passive satellite microwave radiometers,  
518 *IEEE Trans. Geosci. Remote Sens.* **2009**, 47, 3065–3083, doi:10.1109/TGRS.2009.2027012

519 25. El-Nimri, S. F., Lindwood Jones, W., Uhlhorn, E., Ruf, C., Johnson, J., Black, P. An improved C-band ocean  
520 surface emissivity model at hurricane-force wind speeds over a wide range of Earth incidence angles,  
521 *IEEE Geosci. Remote Sens. Lett.* **2010**, 7, 641–645, doi:10.1109/LGRS.2010.2043814.

522 26. Reul N., Tenerelli J., Chapron B., Vandemark D., Quilfen Y., Kerr, Y. SMOS satellite L-band radiometer: A  
523 new capability for ocean surface remote sensing in hurricanes. *Journal of Geophysical Research* **2012**, vol. 117,  
524 C02006, doi: 10.1029/2011JC007474.

525 27. Reul N., Chapron B., Zabolotskikh E., Donion C., Mouche A.A., Tenerelli J., Collard F., Piolle J.F., Fore A.,  
526 Yueh S., Cotton J., Francis P., Quilfen Y., Kudryavtsev V. A new generation of tropical cyclone size  
527 measurements from space. *Bull. Am. Meteorol. Soc.* **2017**, 98: 2367–2385,  
528 <https://doi.org/10.1175/BAMS-D15-00291.1>.

529 28. Zabolotskikh E., Mitnik L. M., Reul N., Chapron B. New Possibilities for Geophysical Parameter Retrievals  
530 Opened by GCOM-W1 AMSR2. *IEEE Journal of Selected Topics in Applied Earth Observations and Remote  
531 Sensing* **2015**, PP(99), 1-14. Publisher's official version : <http://dx.doi.org/10.1109/JSTARS.2015.241651>.

532 29. Fore, A. G., Yueh, S.H., Tang, W., Stiles, B., Hayashi, A.K. Combined Active/Passive Retrievals of Ocean  
533 Vector Wind and Sea Surface Salinity With SMAP. *IEEE Trans. Geosci. Remote Sens.* **2016**, 54(12), 7396-7404.

534 30. Foti, G., Gommenginger, C., Jales, P., Unwin, M., Shaw, A., Robertson, C., Rosell, J. Spaceborne GNSS  
535 reflectometry for ocean winds: First results from the UK TechDemoSat-1 mission. *Geophys. Res.Lett.* **2015**,  
536 vol. 42, no. 13, pp. 5435–5441. <http://dx.doi.org/10.1002/2015GL064204>

537 31. Ruf, C., and Coauthors. New Ocean Winds Satellite Mission to Probe Hurricanes and Tropical Convection.  
538 *Bull. Amer. Meteor. Soc.* **2016**, 97, 385-395, doi:10.1175/BAMS-D-14-00218.1.

539 32. Morris, M., Ruf, C. Determining Tropical Cyclone Surface Wind Speed Structure and Intensity with the  
540 CYGNSS Satellite Constellation. *J. Appl. Meteor. Climatol.* **2017**, doi:10.1175/JAMC-D-16-0375.1

541 33. Holland, G. An Analytic Model of the Wind and Pressure Profiles in Hurricanes. *Monthly Weather Review*  
542 **1980**, 108:1212–1218.

543 34. Willoughby, H.E., Rahn, M.E. Parametric representation of the primary hurricane vortex. Part I:  
544 Observations and evaluation of the Holland (1980) model. *Mon. Wea. Rev.* **2004**, 132, 3033–3048.

545 35. Jelesnianski, C.P., Taylor, A.D. A preliminary view of storm surges before and after storm modifications.  
546 *NOAA Technical Memorandum. ERL WMPO-3, National Oceanic and Atmospheric Administration, U.S.  
547 Department of Commerce* **1973**, pp.33.

548 36. Emanuel, K., Rotunno, R. Self-stratification of tropical cyclone outflow, Part I: Implications for storm  
549 structure, *J. Atmos. Sci.* **2011**, 68, 2236–2249.

550 37. Murty, P.L.N., Bhaskaran, P.K., Gayathri, R., Sahoo, B., Srinivasa Kumar, T., SubbaReddy, B. Numerical  
551 study of coastal hydrodynamics using a coupled model for Hudhud cyclone in the Bay of Bengal,  
552 *Estuarine, Coastal and Shelf Science* **2016**, doi: 10.1016/j.ecss.2016.10.013.

553 38. Powell, M. D., Vickery, P.J., Reinhold, T.A. Reduced drag coefficient for high wind speeds in tropical  
554 cyclones, *Nature* **2003**, 422(6929), 279–283, doi:10.1038/nature01481.

555 39. Willoughby, H. E., Rahn, M. E., Darling, R. W. R. Parametric representation of the primary hurricane  
556 vortex. Part II: A new family of sectionally continuous profiles. *Mon. Weath. Rev.* **2006**, 134, 1102–1120.

557 40. Ruf, C. S., Gleason, S., McKague, D.S. Assessment of CYGNSS Wind Speed Retrieval Uncertainty. *IEEE J.  
558 Sel. Topics Appl. Earth Obs. Remote Sens.* **2018**. DOI:10.1109/JSTARS.2018.2825948.

559 41. Saïd, F., Katzberg, S.J., Soisuvarn, S. Retrieving Hurricane Maximum Winds Using Simulated CYGNSS  
560 Power-Versus-Delay Waveforms. *IEEE Journal of Selected Topics in Applied Earth Observations and Remote  
561 Sensing* **2017**. DOI:10.1109/JSTARS.2017.2695878

562 42. ASCAT Wind Product User Manual, KNMI, De Bit, The Netherlands, **2013**. [Online]. Available:  
563 [http://projects.knmi.nl/scatterometer/publications/pdf/ASCAT\\_Product\\_Manual.pdf](http://projects.knmi.nl/scatterometer/publications/pdf/ASCAT_Product_Manual.pdf)

564 43. Verhoef, A., Portabella, M., and Stoffelen, A. High-resolution ASCAT scatterometer winds near the coast.  
565 *IEEE Trans. Geosci. Remote Sens.* **2012**, vol. 50, no. 7, pp. 2481–2487, doi:10.1109/TGRS.2016.2544835

566 44. Hu, K., Chen, Q., Kimball, S.K. Consistency in hurricane surface wind forecasting : an improved  
567 parametric model. *Nat. Hazards* **2012**, 61, 1029-1050.

568 45. Emanuel, K. *Tropical cyclone energetics and structure*, in Atmospheric Turbulence and Mesoscale  
569 Meteorology, edited by E. Fedorovich, R. Rotunno, and B. Stevens **2004**, pp. 165–192, Cambridge Univ.  
570 Press, Cambridge, U. K., doi:10.1017/CBO9780511735035.010.

571 46. Jelesnianski, C. P., Chen, J., Shaffer, W.A. *SLOSH: Sea, lake, and overland surges from hurricanes*, NOAA Tech.  
572 Rep. **1992** NWS 48, NOAA AOML Library, Miami, Fla.

573 47. Brennan, M.J., Hennon, C.C., Knabb, R.D. The Operational Use of QuikSCAT Ocean Surface Vector Winds  
574 at the National Hurricane Center. *Weather and Forecasting* **2009**, *24*, 621-645.

575 48. Chavas, D. R., Lin, N., Emanuel, K. A model for the complete radial structure of the tropical cyclone wind  
576 field. Part I: Comparison with observed structure. *J. Atmos. Sci.* **2015**, *72*, 3647-3662,  
577 doi:<https://doi.org/10.1175/JAS-D-15-0014.1>

578 49. Zhang, Y., Ye, F., Stanev, E.V., Grashorn, S. Seamless cross-scale modeling with SCHISM. *Ocean Modelling*  
579 **2016**, *102*, 64-81.

580 50. Carrère, L., Lyar, F., Cancet, M., Guillot, A., Roblou, L. FES2012: A new global tidal model taking  
581 advantage of nearly 20 years of altimetry. In: *Paper presented at Proceedings of The Symposium 20 Years of*  
582 *Progress in Radar Altimetry*, **2012**, Venice.

583 51. Saha, S., et al. NCEP Climate Forecast System Version 2 (CFSv2) Monthly Products. Research Data Archive at  
584 the National Center for Atmospheric Research, Computational and Information Systems Laboratory, **2012**,  
585 <https://doi.org/10.5065/D69021ZF>. Accessed 27/10/2017.